Cancer Cell, Volume *32*

Supplemental Information

A Dual Role of Caspase-8 in Triggering and Sensing Proliferation-Associated DNA Damage, a Key Determinant of Liver Cancer Development

Yannick Boege, Mohsen Malehmir, Marc E. Healy, Kira Bettermann, Anna Lorentzen, Mihael Vucur, Akshay K. Ahuja, Friederike Böhm, Joachim C. Mertens, Yutaka Shimizu, Lukas Frick, Caroline Remouchamps, Karun Mutreja, Thilo Kähne, Devakumar Sundaravinayagam, Monika J. Wolf, Hubert Rehrauer, Christiane Koppe, Tobias Speicher, Susagna Padrissa-Altés, Renaud Maire, Jörn M. Schattenberg, Ju-Seong Jeong, Lei Liu, Stefan Zwirner, Regina Boger, Norbert Hüser, Roger J. Davis, Beat Müllhaupt, Holger Moch, Henning Schulze-Bergkamen, Pierre-Alain Clavien, Sabine Werner, Lubor Borsig, Sanjiv A. Luther, Philipp J. Jost, Ricardo Weinlich, Kristian Unger, Axel Behrens, Laura Hillert, Christopher Dillon, Michela Di Virgilio, David Wallach, Emmanuel Dejardin, Lars Zender, Michael Naumann, Henning Walczak, Douglas R. Green, Massimo Lopes, Inna Lavrik, Tom Luedde, Mathias Heikenwalder, and Achim Weber

A

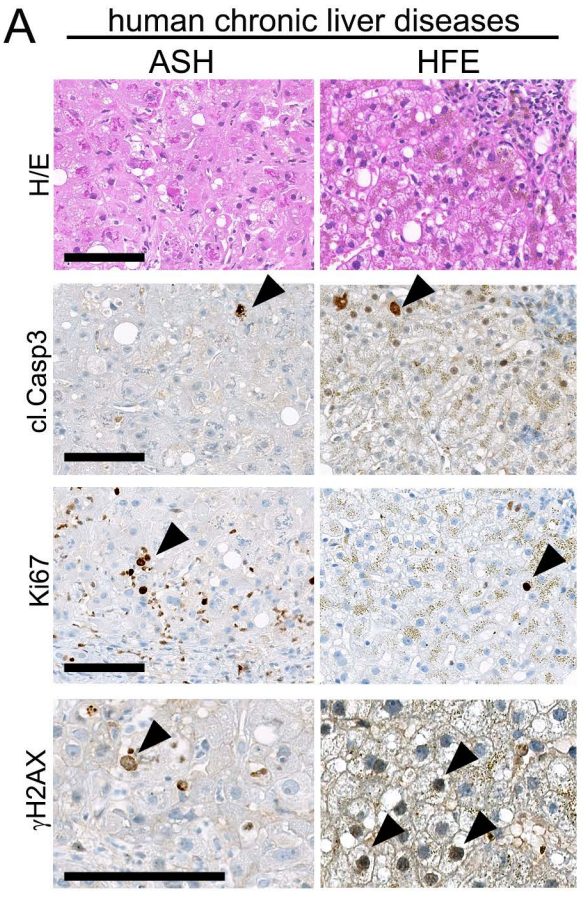

B

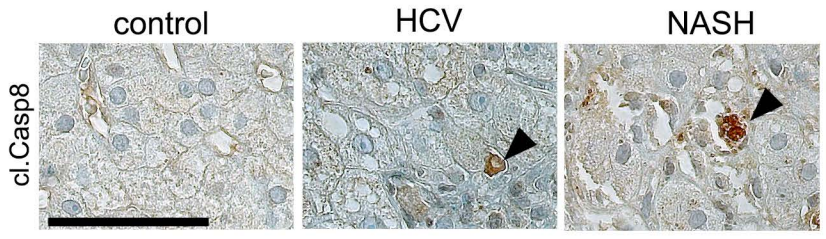

C

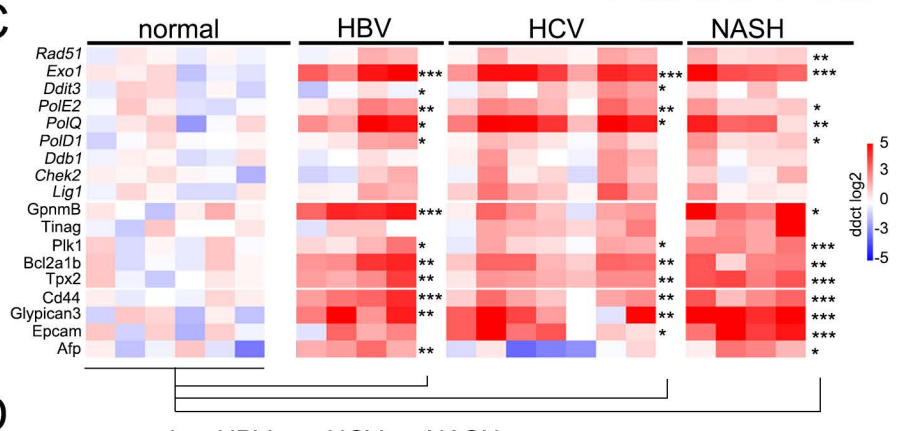

D

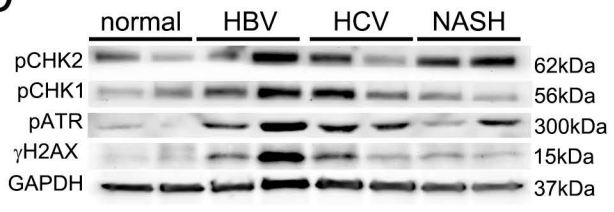

E

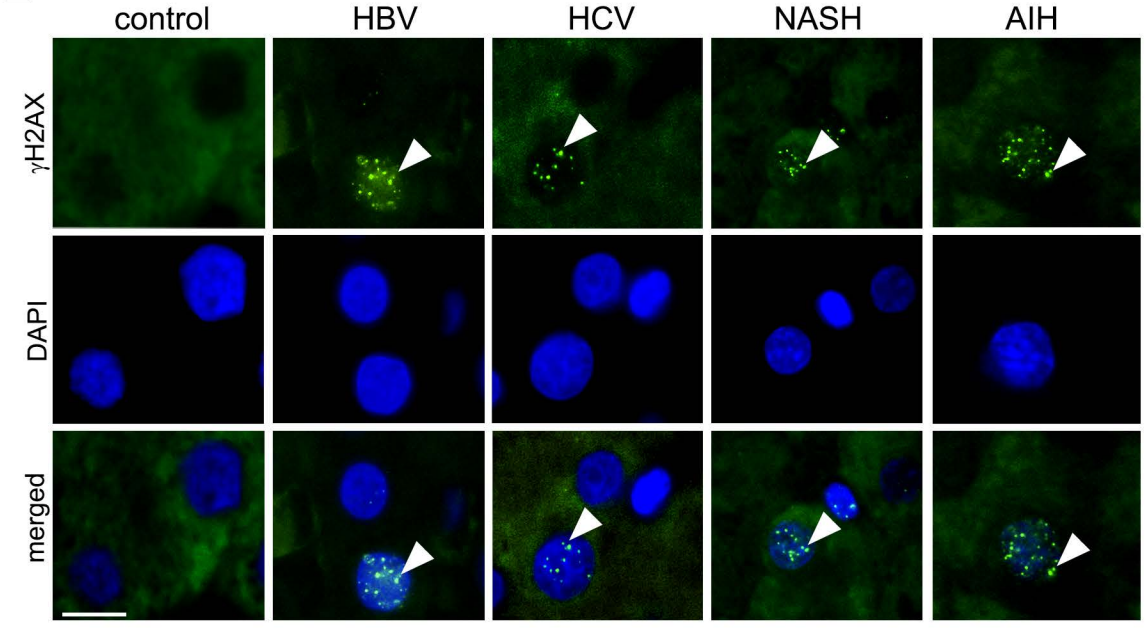

F

	γH2AX positive	γH2AX negative	Fisher's Exact Test
normal	3	14	
HBV	14	1	*p<0.001*
HCV	25	2	*p<0.001*
NASH	18	2	*p<0.001*
AIH	7	1	*p=0.02*

G

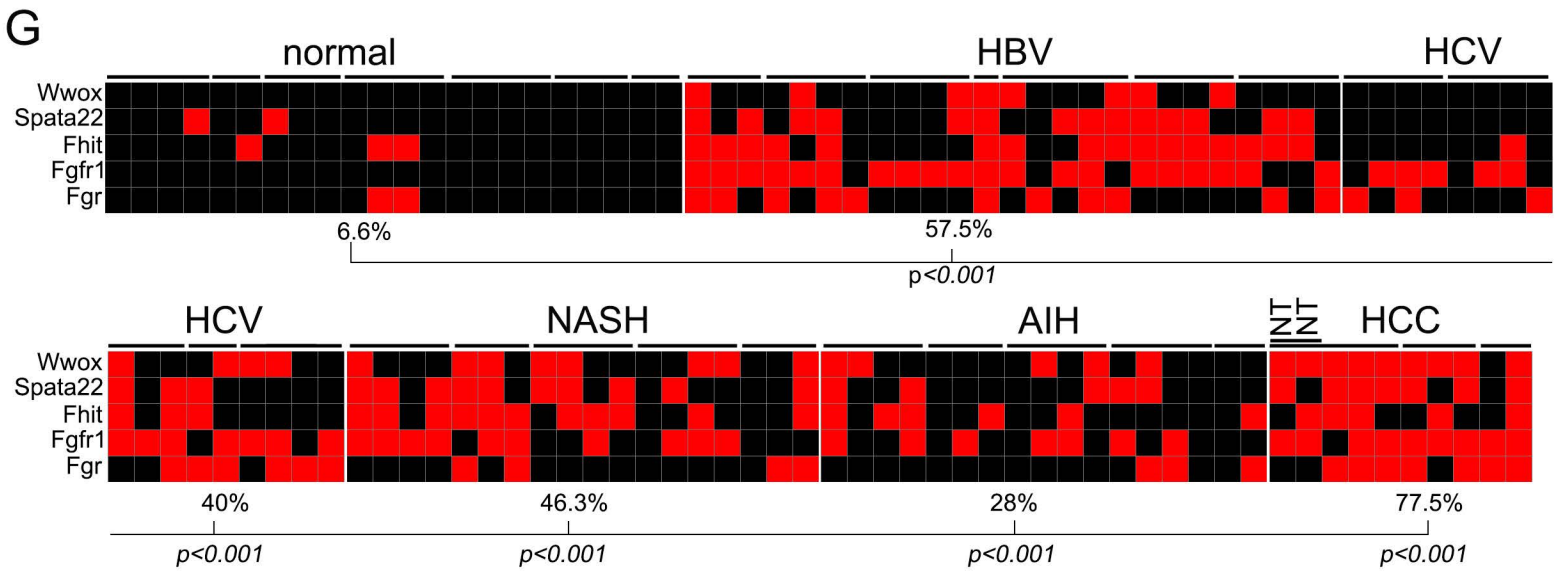

H

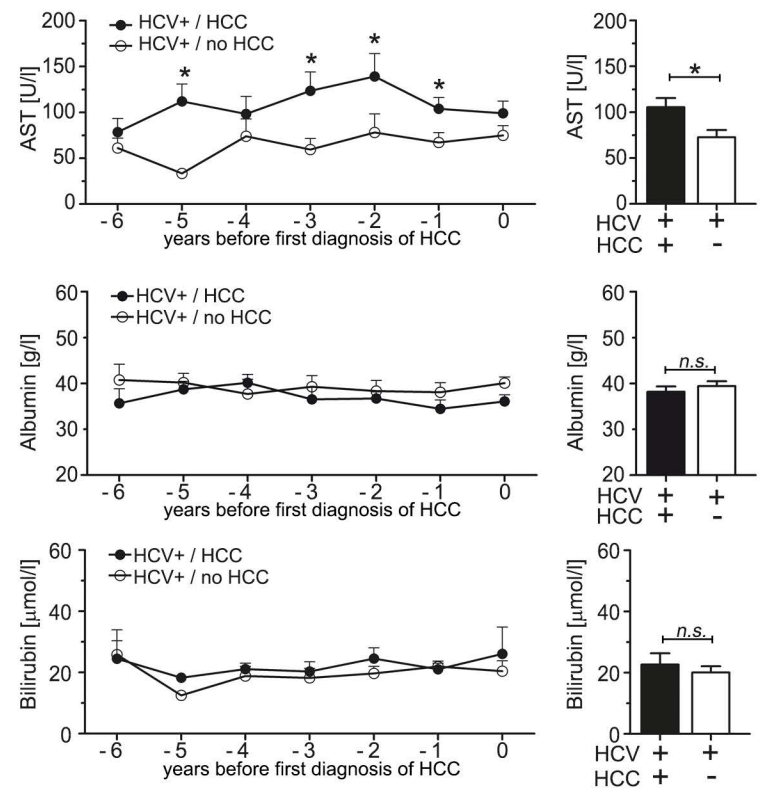

I

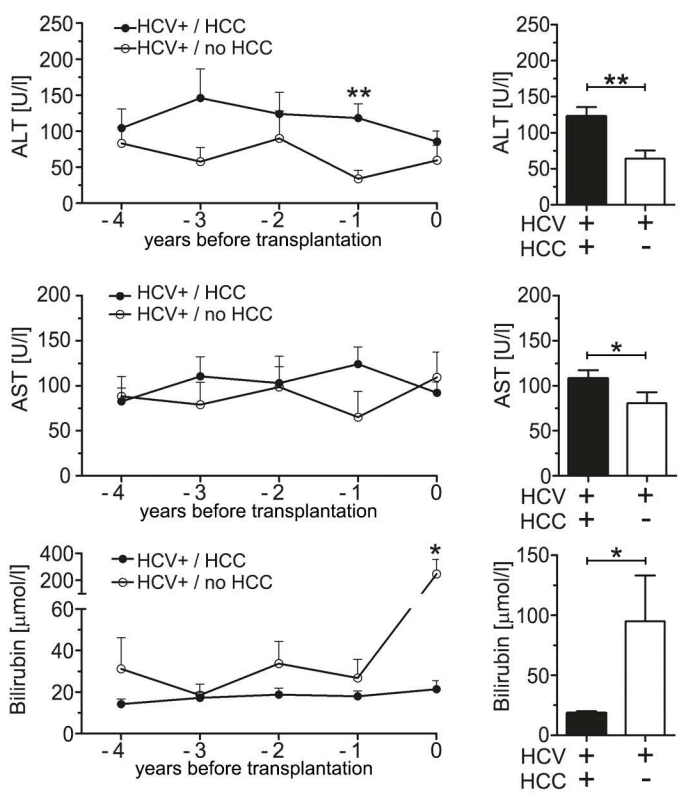

Figure S1, related to Figure 1. DNA damage and genetic instability CLD preceding neoplastic lesions and HCC. (A) Additional human CLD of different etiology including alcoholic steatohepatitis (ASH) and genetic hemochromatosis (HFE) reveal increased levels of apoptosis (cl.Casp3), proliferation (Ki67), and signs of DNA damage (γH2AX). Scale bars: 100 μm. **(B)** Immunohistochemical analysis of cleaved caspase 8 showing positive expression in the livers of HCV-infected patients and NASH patients. Scale bars: 100 μm. **(C)** Increased expression levels of genes associated with DNA repair (e.g. *Rad51, Exo1, PolD1*) in CLD tissue and markers of malignancy (e.g. *CD44, Tpx2, Glypican3*). **(D)** Representative Western blot analyses of CLD tissues (liver biopsies) with increased levels of proteins associated with DNA repair. **(E)** Immunofluorescence staining showing the typical dotted nuclear staining pattern of γH2AX (green) indicative of DNA damage response. DAPI (blue) indicates nuclear staining. Scale bar: 10 μm. **(F)** Semi-quantitative immunohistochemical analysis of γH2AX-positive cells in CLD compared to normal liver. **(G)** Additional CLD tissues showing increased rate of allelic imbalances (AI) reflecting genetic instability detected by TaqMan copy number assay. Each square represents one area of micro-dissected liver tissue and lines indicate different areas of the same liver (red: AI; black: no AI, NT= non-tumor CLD tissue). **(H)** Significantly higher AST, but not albumin or bilirubin levels in HCV patients with HCC development compared to matched HCV patients without HCC development of the same cohort. **(I)** Significantly higher ALT and AST, but lower bilirubin levels (due to less frequent terminal liver failure) in liver transplantation patients with HCC development compared to matched patients without HCC development of the same cohort. In (H) and (I), data are presented as mean ± SEM. Statistical significance was calculated using Student's *t*-test (H,I). **p* < 0.05; ***p* < 0.01.

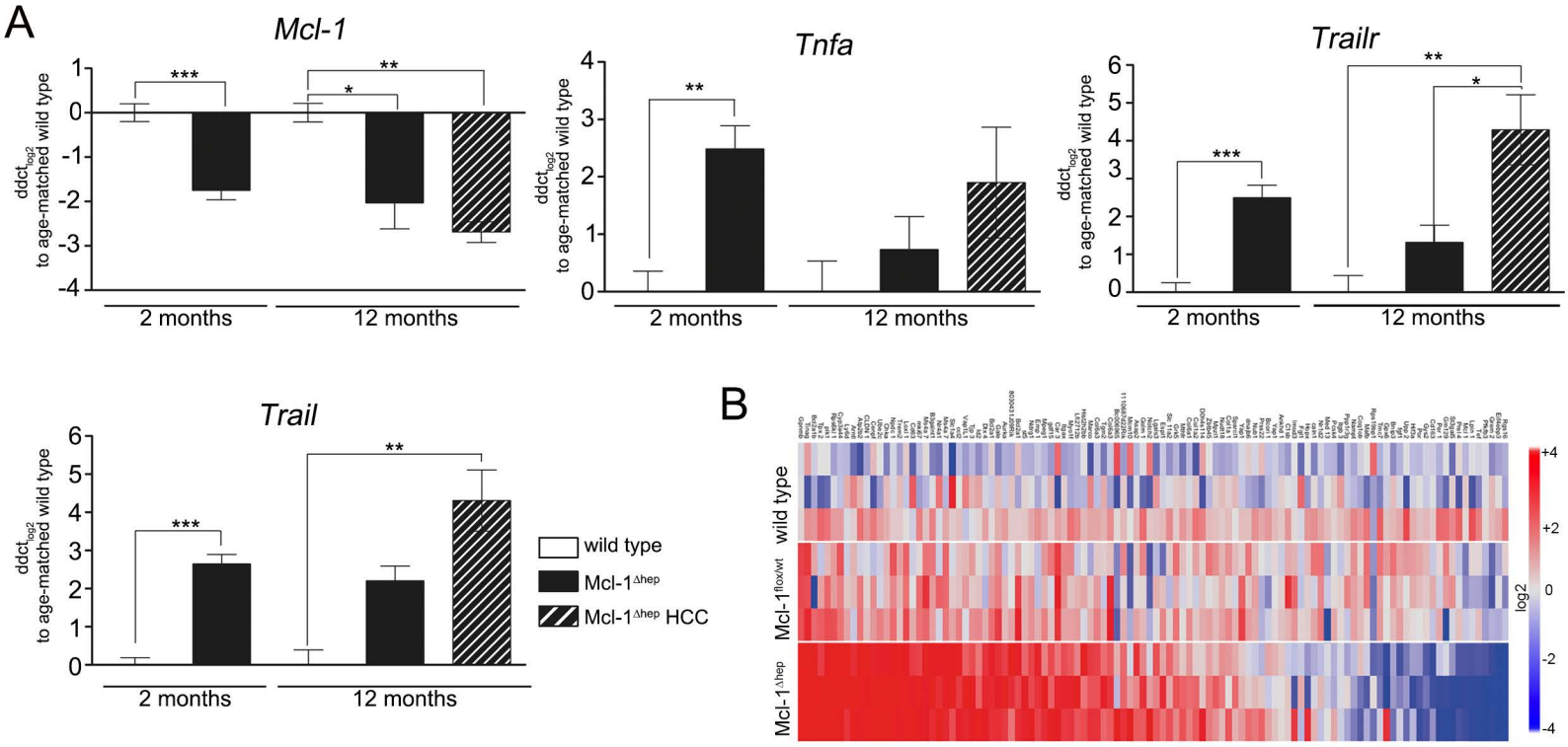
A
Mcl-1
Tnfa
Trailr
Trail
ddct log2 to age-matched wild type
2 months
12 months
wild type
Mcl-1Δhep
Mcl-1Δhep HCC
B
wild type
Mcl-1flox/wt
Mcl-1Δhep
log2
+4
+2
0
-2
-4

Figure S2, related to Figure 2. Risk of HCC development correlates with apoptosis and DNA damage in Mcl-1$^{\Delta hep}$ mice. (A) Gene expression analysis by qPCR for *Mcl-1*, death receptor ligands (*Tnfα, Trail*) and death receptor (*Trailr*) of murine liver tissue at either 2 or 12 months of age. **(B)** Deregulated genes validated by qPCR in 2-months-old homozygous and hemizygous Mcl-1$^{\Delta hep}$ mice and controls (n=3 per group). In (A), data are presented as mean ± SEM. Statistical significance was calculated using Student's *t*-test. **p* < 0.05; ***p* < 0.01; ****p* < 0.001.

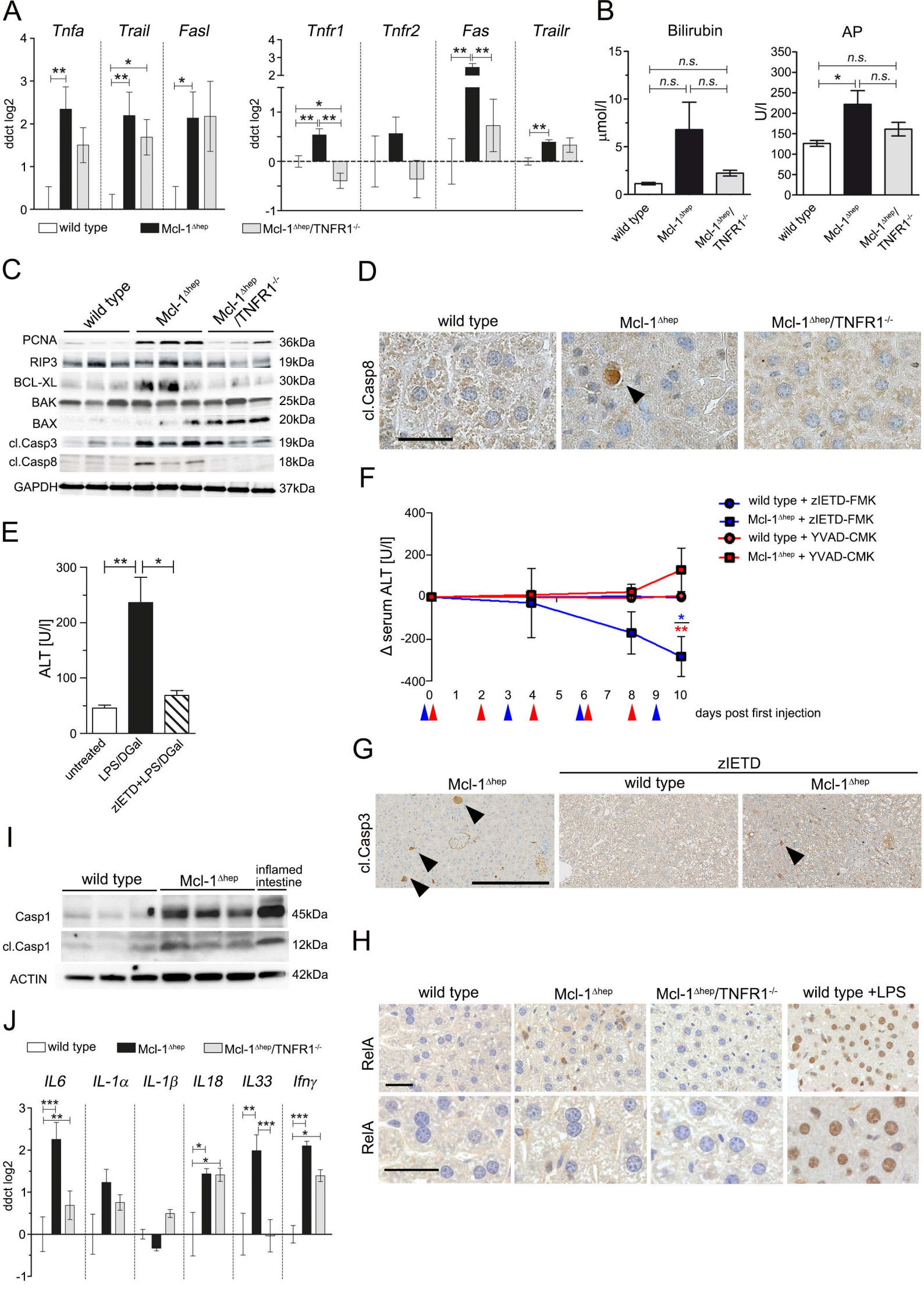
A
Tnfa
Trail
Fasl
Tnfr1
Tnfr2
Fas
Trailr
ddct log2
wild type
Mcl-1Δhep
Mcl-1Δhep/TNFR1-/-
B
Bilirubin
AP
µmol/l
U/l
n.s.
wild type
Mcl-1Δhep
Mcl-1Δhep/ TNFR1-/-
C
wild type
Mcl-1Δhep
Mcl-1Δhep /TNFR1-/-
PCNA
RIP3
BCL-XL
BAK
BAX
cl.Casp3
cl.Casp8
GAPDH
36kDa
19kDa
30kDa
25kDa
20kDa
19kDa
18kDa
37kDa
D
wild type
Mcl-1Δhep
Mcl-1Δhep/TNFR1-/-
cl.Casp8
E
ALT [U/l]
untreated
LPS/DGal
zIETD+LPS/DGal
F
Δ serum ALT [U/l]
wild type + zIETD-FMK
Mcl-1Δhep + zIETD-FMK
wild type + YVAD-CMK
Mcl-1Δhep + YVAD-CMK
days post first injection
G
zIETD
Mcl-1Δhep
wild type
Mcl-1Δhep
cl.Casp3
H
wild type
Mcl-1Δhep
Mcl-1Δhep/TNFR1-/-
wild type +LPS
RelA
RelA
I
wild type
Mcl-1Δhep
inflamed intestine
Casp1
cl.Casp1
ACTIN
45kDa
12kDa
42kDa
J
wild type
Mcl-1Δhep
Mcl-1Δhep/TNFR1-/-
IL6
IL-1α
IL-1β
IL18
IL33
Ifnγ
ddct log2

Figure S3, related to Figure 3. Reduced apoptosis, proliferation, and tumor development in Mcl-1$^{\Delta hep}$/TNFR1$^{-/-}$ mice. (A) Significant changes in the expression of death receptors (*Tnfr1, Tnfr2, Fas, Trailr*) and ligands (*Tnfα, Trail, Fasl*) comparing Mcl-1$^{\Delta hep}$ (n=7), Mcl-1$^{\Delta hep}$/TNFR1$^{-/-}$ mice (n=5) and wild type mice (n=7). **(B)** Bilirubin and AP in 2-months-old Mcl-1$^{\Delta hep}$ (n=16), Mcl-1/TNFR1$^{-/-}$ (n=10) and wild type mice (n=8). **(C)** Western blot analysis of proliferation and apoptosis proteins in livers of Mcl-1$^{\Delta hep}$/TNFR1$^{-/-}$ mice, compared to Mcl-1$^{\Delta hep}$ mice. **(D)** Immunohistochemistry for cleaved caspase 8 in livers of 2-months-old wild type control mice, Mcl-1$^{\Delta hep}$ mice and Mcl-1$^{\Delta hep}$/TNFR1$^{-/-}$ mice. Scale bar: 50 μm. **(E)** ALT levels of wild type mice 4 h post LPS/DGal induction of hepatocyte apoptosis, with or without zIETD pre-treatment (n=3 mice per group). **(F)** 6-8 week old Mcl-1$^{\Delta hep}$ mice treated with the caspase 8-specific inhibitor zIETD (n=3 wild type and n=4 Mcl-1$^{\Delta hep}$ mice) showed a significant reduction in serum ALT levels. Treating age-matched Mcl-1$^{\Delta hep}$ mice with the caspase 1 inhibitor YVAD-CMK (n=3 wild type and n=5 Mcl-1$^{\Delta hep}$ mice) had no effect on serum levels of ALT. Injection time-points are marked with blue arrowheads for zIEDT treated mice or red arrowheads for YVAD-CMK treated mice. **(G)** IHC for cleaved caspase 3 in zIETD treated wild type and Mcl-1$^{\Delta hep}$ mice as well as untreated Mcl-1$^{\Delta hep}$ mice. Scale bar: 250 μm. **(H)** Immunohistochemistry for RelA demonstrates no obvious RelA nuclear translocation in livers of Mcl-1$^{\Delta hep}$ and Mcl-1$^{\Delta hep}$/TNFR1$^{-/-}$ mice. Scale bars: 50 μm. **(I)** Western blot analysis from whole liver protein extracts analysing cleaved caspase 1 expression in wild type or Mcl-1$^{\Delta hep}$ mice. **(J)** Cytokine expression analysis by qPCR from liver homogenates of 2-months-old Mcl-1$^{\Delta hep}$ mice, Mcl-1$^{\Delta hep}$/TNFR1$^{-/-}$ mice and wild type control mice. Data presented as bar charts (A), (B), (E) and (J) represent mean values ± SEM. Data presented as line graph (F) represents mean values ± SEM. Statistical significance was calculated using ANOVA with Bonferroni correction (A) and (J), Student's *t*-test (B), (E) or Mann-Whitney U test (F). *$p < 0.05$; **$p < 0.01$; ***$p < 0.001$.

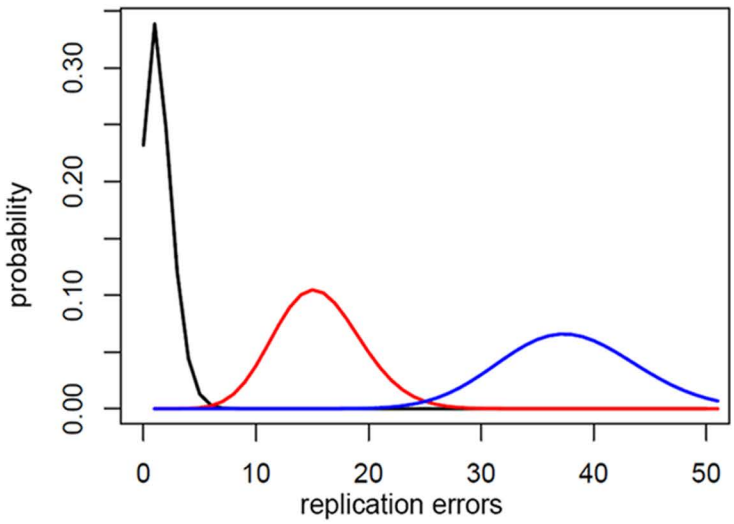
probability
0.00
0.10
0.20
0.30
0
10
20
30
40
50
replication errors

Figure S4, related to Figure 3. Hepatocyte apoptosis and HCC development. Replication errors in relation to the rate of hepatocyte proliferation. A rough calculation of replication error rates depending on the replicative activity in wild type mice (black) as well as Mcl-1$^{\Delta hep}$ mice with low transaminase levels and corresponding low proliferative activity (red) or Mcl-1$^{\Delta hep}$ mice with high transaminase levels and corresponding high proliferative activity (blue). The expected number of replications errors after 1 year of is 1.46 for wild type mice (black line), 14.6 for Mcl-1$^{\Delta hep}$ mice with low hepatocyte proliferative activity, and 36.8 for Mcl-1$^{\Delta hep}$ mice with high hepatocyte proliferative activity (blue line).

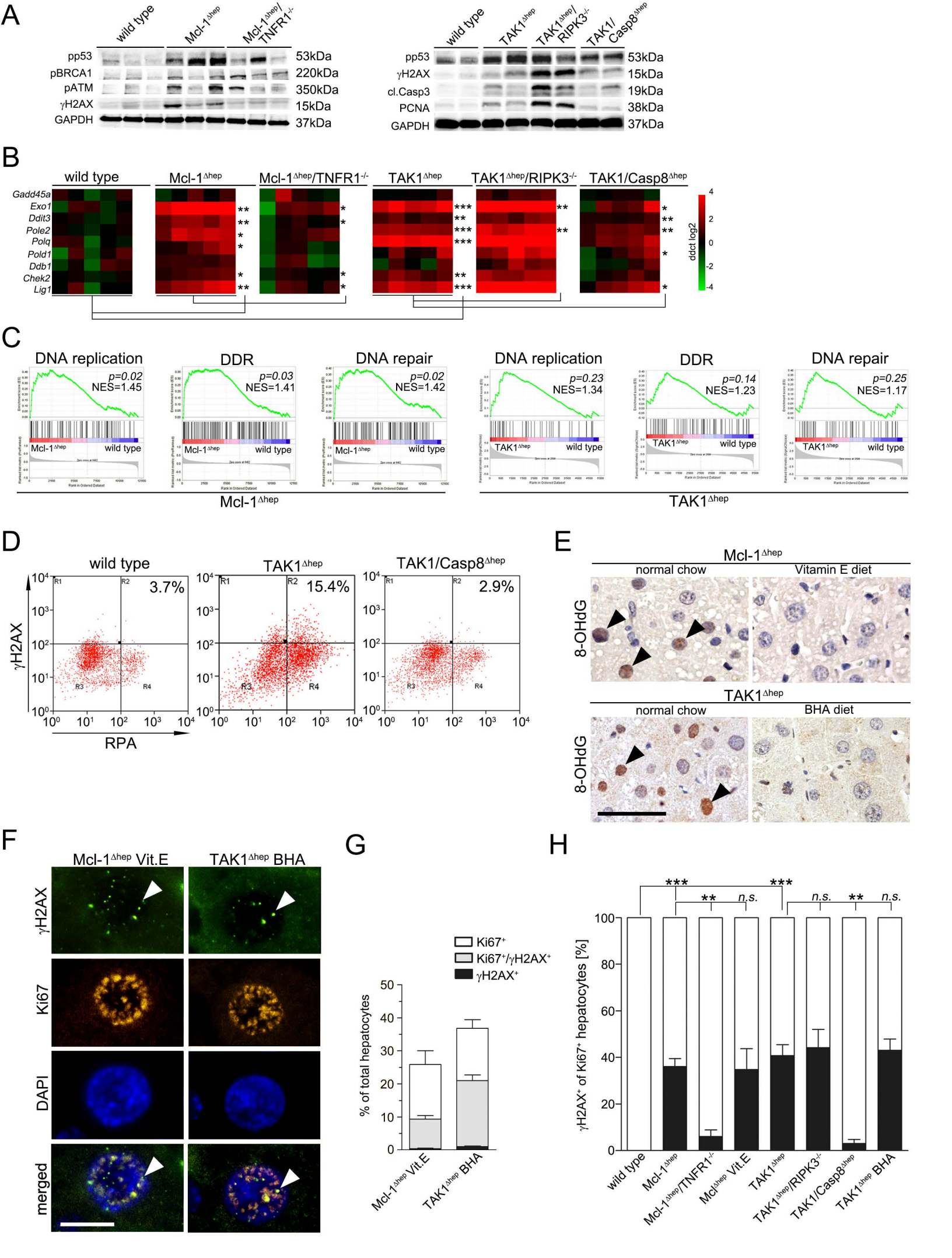
A
wild type
Mcl-1Δhep
Mcl-1Δhep/TNFR1-/-
pp53
pBRCA1
pATM
γH2AX
GAPDH
53kDa
220kDa
350kDa
15kDa
37kDa
wild type
TAK1Δhep
TAK1Δhep/RIPK3-/-
TAK1/Casp8Δhep
pp53
γH2AX
cl.Casp3
PCNA
GAPDH
53kDa
15kDa
19kDa
38kDa
37kDa
B
wild type
Mcl-1Δhep
Mcl-1Δhep/TNFR1-/-
TAK1Δhep
TAK1Δhep/RIPK3-/-
TAK1/Casp8Δhep
Gadd45a
Exo1
Ddit3
Pole2
Polq
Pold1
Ddb1
Chek2
Lig1
ddct log2
4
2
0
-2
-4
C
DNA replication
DDR
DNA repair
p=0.02
NES=1.45
p=0.03
NES=1.41
p=0.02
NES=1.42
Mcl-1Δhep
wild type
Mcl-1Δhep
DNA replication
DDR
DNA repair
p=0.23
NES=1.34
p=0.14
NES=1.23
p=0.25
NES=1.17
TAK1Δhep
wild type
TAK1Δhep
D
wild type
TAK1Δhep
TAK1/Casp8Δhep
3.7%
15.4%
2.9%
R1
R2
R3
R4
γH2AX
RPA
E
Mcl-1Δhep
normal chow
Vitamin E diet
8-OHdG
TAK1Δhep
normal chow
BHA diet
8-OHdG
F
Mcl-1Δhep Vit.E
TAK1Δhep BHA
γH2AX
Ki67
DAPI
merged
G
Ki67+
Ki67+/γH2AX+
γH2AX+
% of total hepatocytes
Mcl-1Δhep Vit.E
TAK1Δhep BHA
H
γH2AX+ of Ki67+ hepatocytes [%]
***
**
n.s.
wild type
Mcl-1Δhep
Mcl-1Δhep/TNFR1-/-
Mcl1Δhep Vit.E
TAK1Δhep
TAK1Δhep/RIPK3-/-
TAK1/Casp8Δhep
TAK1Δhep BHA

Figure S5, related to Figure 4. DNA damage and genetic instability in Mcl-1$^{\Delta hep}$ and TAK1$^{\Delta hep}$ mice and intercrossings. (A) Western blot analysis shows reduced activation of DNA damage and DNA repair protein levels in liver homogenates from Mcl-1$^{\Delta hep}$/TNFR1$^{-/-}$ mice when compared to TAK1$^{\Delta hep}$ mice. **(B)** Heat map analysis illustrates reduced expression of DNA damage and DNA repair-associated genes (qPCR) in livers of Mcl-1$^{\Delta hep}$/TNFR1$^{-/-}$ mice when compared to Mcl-1$^{\Delta hep}$ mice. A similar effect was observed in livers of TAK1/Casp8$^{\Delta hep}$ mice compared to TAK1$^{\Delta hep}$ controls. **(C)** GSEA reveals statistically significant enrichment of genes associated with DNA replication, DNA damage response and DNA repair in Mcl-1$^{\Delta hep}$ and TAK1$^{\Delta hep}$ mice, respectively. (NES= normalized enrichment score). **(D)** Intracellular hepatocyte FACS analysis for γH2AX and RPA showing reduced DNA damage in TAK1/ Casp8$^{\Delta hep}$ mice compared to TAK1$^{\Delta hep}$. (2-4 mice per genotype; average percentage of γH2AX $^{+}$/RPA^{+} cells indicated). **(E)** Livers of Mcl-1$^{\Delta hep}$ and TAK1$^{\Delta hep}$ mice on normal chow but not on antioxidant diets show 8-OHdG positive hepatocytes, indicating oxidative stress. Scale bar: 50 μm. **(F)** and **(G)** Livers of mice on antioxidant diet: Mcl-1$^{\Delta hep}$ mice on a Vitamin E supplemented and TAK1$^{\Delta hep}$ mice on a BHA supplemented diet do not have reduced number of hepatocytes positive for γH2AX and Ki67. Scale bar (F): 10 μm. **(H)** Summary of γH2AX positivity of hepatocytes as percentage of proliferating (Ki67-positive) hepatocytes for all genotypes and experiments. **(A)**-**(F)**: Mcl-1$^{\Delta hep}$ mice and intercrossings analyzed at 2 months; TAK1$^{\Delta hep}$ mice and intercrossings analyzed at 6 weeks. Data presented as bar charts (G) and (H) represent mean values ± SEM. Statistical significance was determined using ANOVA with Bonferroni correction (H). $^{**}p < 0.01$; $^{***}p < 0.001$.

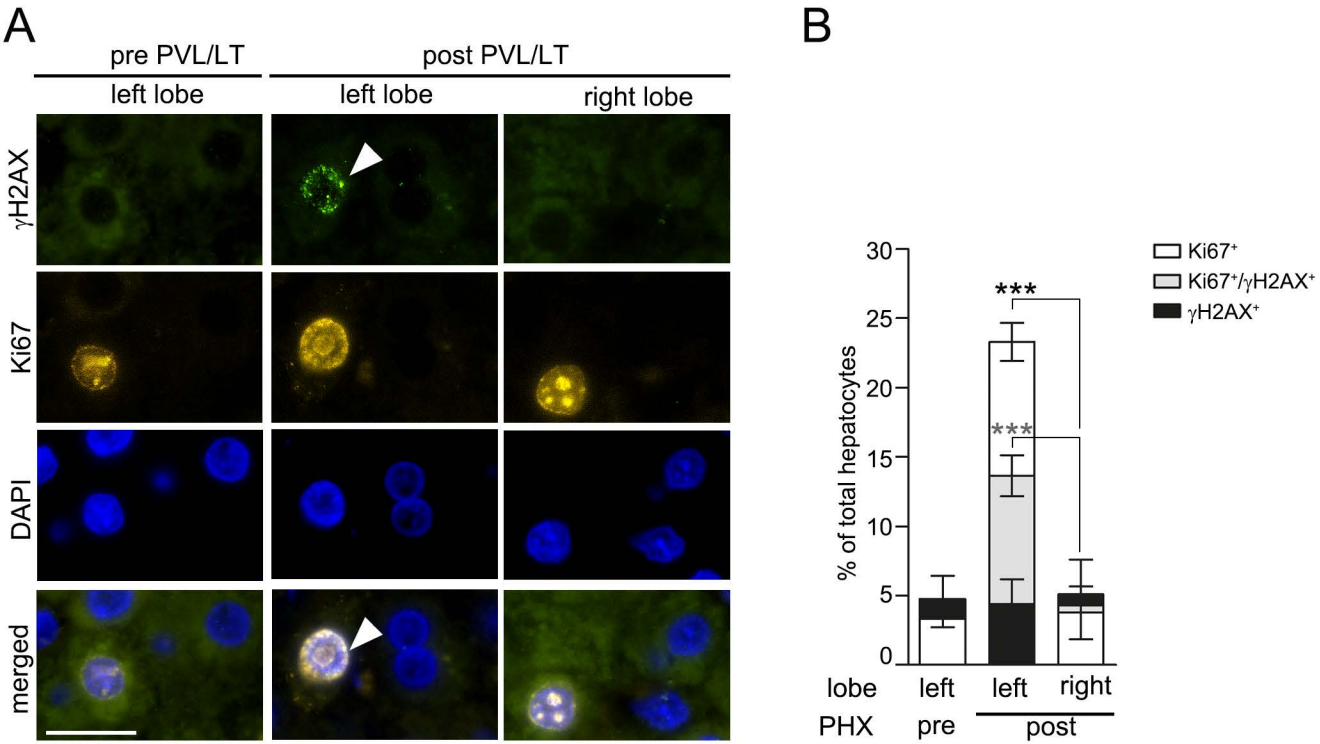
A
pre PVL/LT
post PVL/LT
left lobe
left lobe
right lobe
γH2AX
Ki67
DAPI
merged
B
Ki67+
Ki67+/γH2AX+
γH2AX+
% of total hepatocytes
30
25
20
15
10
5
0
***
***
lobe
left
left
right
PHX
pre
post

Figure S6, related to Figure 5. Hyperproliferation-induced DNA damage after partial hepatectomy (PHX) is impaired in right portal vein ligation and liver transection (PVL/LT) patients. (A) IF staining and **(B)** quantification for Ki67 and γH2AX of hepatocytes in liver biospies of patients prior to and after PVL/LT demonstrating a significant increase in γH2AX/ Ki67-double positive hepatocytes in the regenerating liver on the left side compared to right. (Scale bar (A): 20 μm). Data presented as bar charts (B) represents mean values ± SEM. Statistical significance was calculated using ANOVA with Bonferroni correction. ** $p < 0.01$; *** $p < 0.001$.

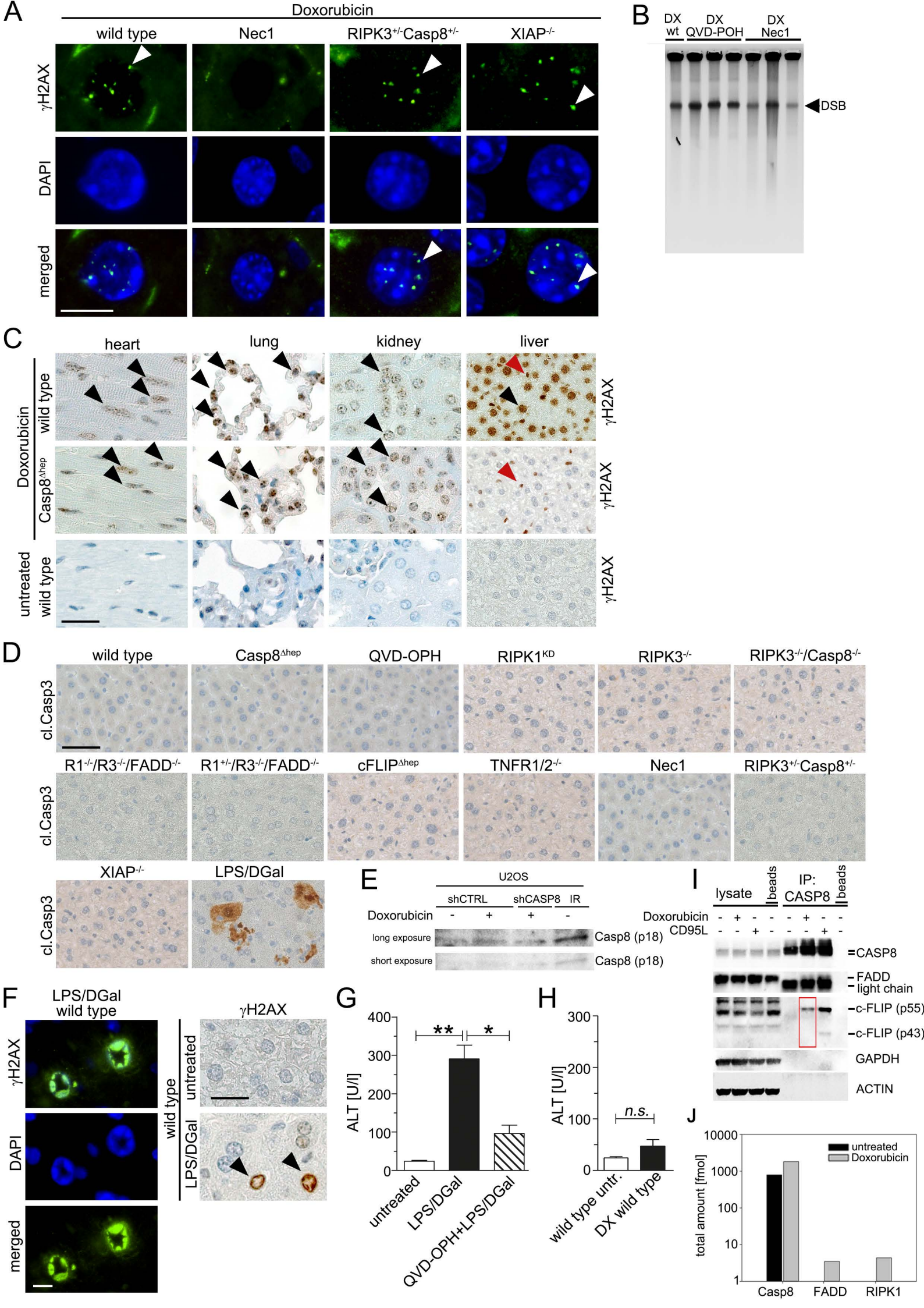
A
Doxorubicin
wild type
Nec1
RIPK3+/-Casp8+/-
XIAP-/-
γH2AX
DAPI
merged
B
DX wt
DX QVD-POH
DX Nec1
DSB
C
heart
lung
kidney
liver
Doxorubicin
wild type
Casp8ΔHep
untreated wild type
γH2AX
D
wild type
Casp8ΔHep
QVD-OPH
RIPK1KD
RIPK3-/-
RIPK3-/-/Casp8-/-
R1-/-/R3-/-/FADD-/-
R1+/-/R3-/-/FADD-/-
cFLIPΔHep
TNFR1/2-/-
Nec1
RIPK3+/-Casp8+/-
XIAP-/-
LPS/DGal
cl.Casp3
E
U2OS
shCTRL
shCASP8
IR
Doxorubicin
long exposure
short exposure
Casp8 (p18)
I
lysate
beads
IP: CASP8
Doxorubicin
CD95L
CASP8
FADD light chain
c-FLIP (p55)
c-FLIP (p43)
GAPDH
ACTIN
F
LPS/DGal wild type
γH2AX
DAPI
merged
wild type
untreated
LPS/DGal
G
ALT [U/l]
**
*
untreated
LPS/DGal
QVD-OPH+LPS/DGal
H
ALT [U/l]
n.s.
wild type untr.
DX wild type
J
total amount [fmol]
untreated
Doxorubicin
Casp8
FADD
RIPK1

Figure S7, related to Figure 6. Casp8, RIPK1, FADD and c-FLIP are crucial for DDR in hepatocytes upon doxorubicin treatment. (A) γH2AX staining of doxorubicin-treated wild type mice or Nec1-treated wild type mice (n=6), $RIPK1^{+/-}Casp^{+/-}$ (n=7) and $XIAP^{-/-}$ mice (n=7). Scale bar: 10 μm. **(B)** DNA strand breaks visualized by PFGE in Nec1 and QVD-OPH pre-treated wild type mice 12 h after doxorubicin challenge. **(C)** γH2AX positivity 12h post doxorubicin injection in heart, lung, kidney and liver in wild type control or $Casp8^{\Delta hep}$ mice. Scale bars: 50 μm. **(D)** IHC for cleaved caspase 3 in wild type mice as well as different knock-out mice upon doxorubicin treatment. As positive control LPS/DGal treated wild type mice were analyzed. Scale bar: 50 μm. **(E)** Western blot analysis for cleaved caspase 8 30 minutes post doxorubicin treatment (1μM). **(F)** Hepatocytes displaying nuclear fragmentation and condensation indicative of apoptosis in livers of LPS/DGal-treated wild type mice shown as controls by immunofluorescence and IHC. Scale bars: 10 μm (left) and 50 μm (right). **(G)** Aminotransferase levels of wild type control mice 4 h post LPS/DGal induction of hepatocyte apoptosis, with or without QVD-OPH pre-treatment (n=3 mice per group). **(H)** Aminotransferase levels reveal no hepatotoxicity upon DX treatment as measured by serum levels of ALT. **(I)** Immunoprecipitation with anti-caspase 8 antibody and immuno blotting of lysates 1h after doxorubicin (5 μM) treatment. Red box indicates caspase 8 and c-Flip interaction following doxorubicin treatment. **(J)** Mass Spec analysis of the precipitates with caspase 8 antibodies. Data presented as bar charts (G) and (H) represent mean values ± SEM. Statistical significance was calculated using Student's *t*-test (G) and (H). **p* < 0.05; ***p* < 0.01.

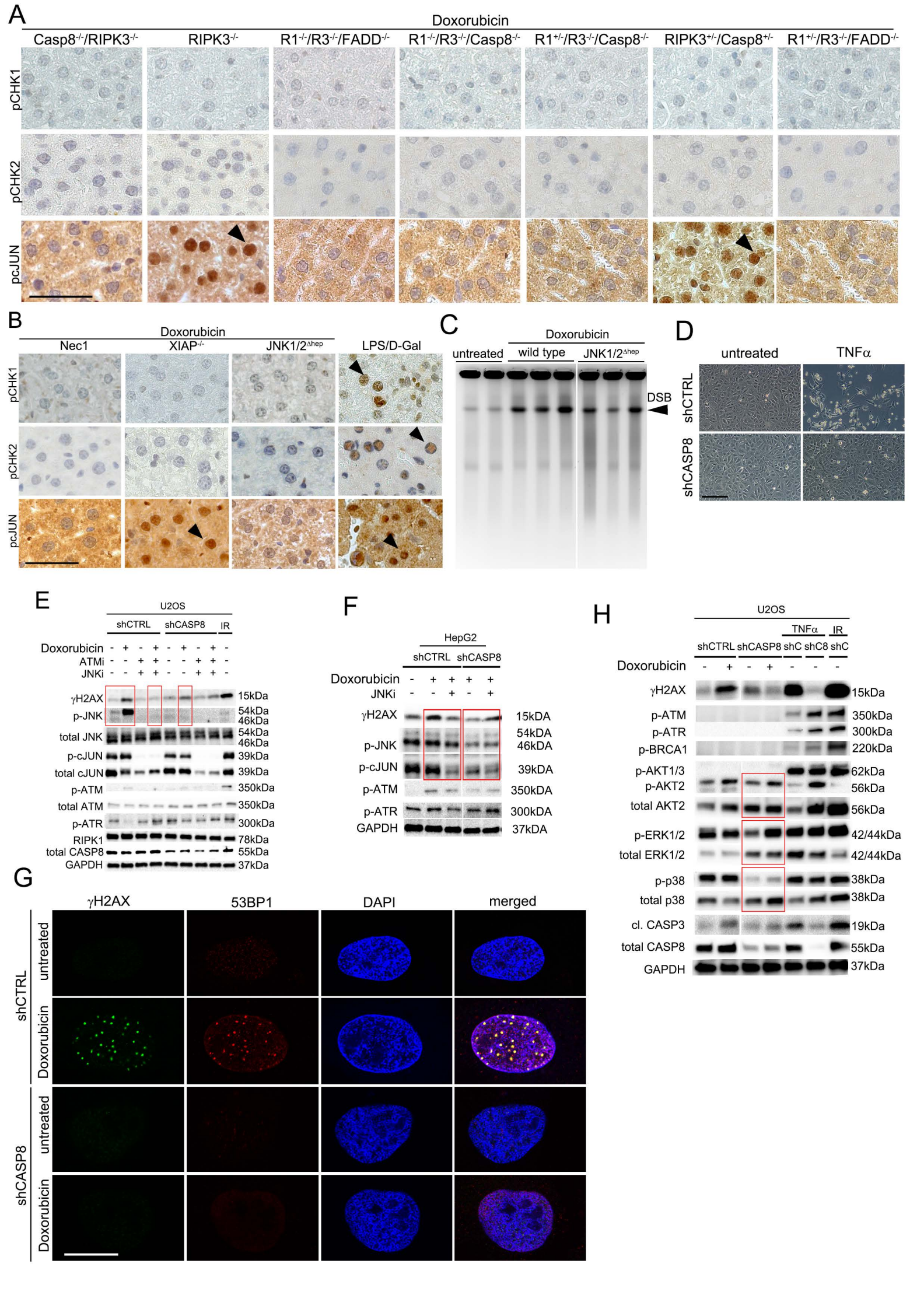
A
Doxorubicin
Casp8-/-/RIPK3-/-
RIPK3-/-
R1-/-/R3-/-/FADD-/-
R1-/-/R3-/-/Casp8-/-
R1+/-/R3-/-/Casp8-/-
RIPK3+/-/Casp8+/-
R1+/-/R3-/-/FADD-/-
pCHK1
pCHK2
pcJUN
B
Doxorubicin
Nec1
XIAP-/-
JNK1/2Δhep
LPS/D-Gal
C
Doxorubicin
untreated
wild type
JNK1/2Δhep
DSB
D
untreated
TNFα
shCTRL
shCASP8
E
U2OS
shCTRL
shCASP8
IR
Doxorubicin
ATMi
JNKi
γH2AX
p-JNK
total JNK
p-cJUN
total cJUN
p-ATM
total ATM
p-ATR
RIPK1
total CASP8
GAPDH
15kDa
54kDa
46kDa
39kDa
350kDa
300kDa
78kDa
55kDa
37kDa
F
HepG2
shCTRL
shCASP8
Doxorubicin
JNKi
γH2AX
p-JNK
p-cJUN
p-ATM
p-ATR
GAPDH
15kDA
54kDA
46kDA
39kDA
350kDA
300kDA
37kDA
H
U2OS
TNFα
IR
shCTRL
shCASP8
shC
shC8
shC
Doxorubicin
γH2AX
p-ATM
p-ATR
p-BRCA1
p-AKT1/3
p-AKT2
total AKT2
p-ERK1/2
total ERK1/2
p-p38
total p38
cl. CASP3
total CASP8
GAPDH
15kDa
350kDa
300kDa
220kDa
62kDa
56kDa
56kDa
42/44kDa
42/44kDa
38kDa
38kDa
19kDa
55kDa
37kDa
G
γH2AX
53BP1
DAPI
merged
shCTRL
shCASP8
untreated
Doxorubicin

Figure S8, related to Figure 7. JNK is a downstream mediator of caspase 8, c-FLIP and RIPK1-dependent DNA damage resonse *in vivo* and *in vitro.* **(A)** and **(B)** Immuno staining for pCHK1, pCHK2 and pcJun in several knock-out mice, respectively. Wild type control mice treated with LPS/DGal **(B)** for the induction of hepatocyte cell death were used as positive controls. Black arrow heads: pcJUN-positive hepatocytes. Scale bars (A) and (B): 50 μm. **(C)** DNA double strand breaks visualized by PFGE in hepatocytes from untreated wild type control mice, as well as wild type control mice and JNK1/2$^{\Delta hep}$ mice following 12 hours doxorubicin treatment. **(D)** Increased cell death in shCTRL cells (U2OS) which was absent or strongly reduced in shCASP8 cells (visualized by apoptotic morphology, phase contrast microscopy) in response to TNFα treatment (10ng/ml) at 48h. Scale bar: 500 μm. **(E)** Analysis of DDR signaling by Western blotting of doxorubicin treated shCTRL or shCASP8 U2OS cells pre-treated with JNK inhibitor (SP600125) and ATM inhibitor (Ku-55933), or untreated as control. Cells were pretreated with both inhibitors for 4h and analyzed by Western blotting 30min post doxorubicin administration (1μM). As control, cells 2h post irradiation (10Gy) were used. GAPDH was probed as a loading control. Red boxes illustrate differences in γH2AX and pJNK activation post doxorubicin treatment. **(F)** Doxorubicin treatment of HepG2 revealed substance- and cell line-independent, but caspase 8-dependent JNK activity and cJUN and γH2AX phosphorylation upon induction of DSB. Western blotting was performed 30 min post DSB induction. Red boxes illustrate differences in γH2AX, pJNK or pcJUN post doxorubicin treatment. **(G)** IF staining and confocal imaging for 53BP1 and γH2AX of U2OS cells 30 min post doxorubicin administration (1μM) revealing lack of 53BP1-positive foci formation in shCASP8cells in contrast to doxorubicin-treated shCTRLcells. DAPI (blue) staining indicates nuclear staining. Scale bar: 10 μm. **(H)** Western blot analyses for MAPK and PI3K signaling pathways revealed lower p-p38 and p-ERK1/2 baseline activation in untreated and higher total amounts of ERK1/2, p38 and AKT2 as wells as impaired p38 activation in doxorubicin-treated shCASP8 cells, compared to doxorubicin-treated shCTRL cells. Red boxes illustrate differences between shCTRL and shCASP8 cells in p-AKT2, AKT2, p-ERK1/2, ERK1/2, p-p38 or p38. Irrelevant lanes omitted from PFGE analysis displayed in (C) and western blot analysis

displayed in (F) and (H). Areas where lanes were omitted are indicated by white space between lanes.

	Liver regeneration at 8 weeks				HCC incidence
	apoptosis	proliferation	DDR	AI	
wild type	-	-	-	-	0%
Mcl-1$^{\Delta hep}$	+	+	+	+	50%
Mcl-1$^{\Delta hep}$/TNFR1$^{-/-}$	+/-	+/-	+/-	+/-	28.2%
	Liver regeneration at 6 weeks				HCC incidence
	apoptosis	proliferation	DDR	AI	
TAK1$^{\Delta hep}$	++	++	++	++	100%
TAK1$^{\Delta hep}$/RIPK3$^{-/-}$	++	++	++	++	100%
TAK1/Casp8$^{\Delta hep}$	-	+/-	-	+/-	0%

Table S1, related to Methods. Mouse strains and intercrossings. Liver damage of mice at the indicated age and tumor incidence analyzed at 12 months of age for Mcl-$1^{\Delta hep}$ and Mcl-$1^{\Delta hep}$/TNFR$1^{-/-}$ mice and 33-35 weeks of age for TAK$1^{\Delta hep}$ mice and intercrossings. AI = allelic imbalances at chromosomal fragile sites. DDR = DNA damage response. "++" indicates significantly increased levels of hepatocytes positive for cl.Casp3, Ki67 or γH2AX, "+/-" indicates slightly elevated levels and "-" indicates level comparable to wild type controls.